The Brain Watching Itself: Identifying Brain Tumors with Spiking Neural Networks

Namita Achyuthan
Dept. of CSE(AIML)
PES University
Bengaluru, India
namitaachyuthan@gmail.com

Bhaskarjyoti Das
Dept. of CSE(AIML)
PES University
Bengaluru, India
bhaskarjyoti01@gmail.com

***Abstract*—This study investigates the application of Spiking Neural Networks (SNNs) in Magnetic Resonance Imaging (MRI) classification to explore their potential as an efficient, biologically inspired alternative to traditional convolutional models. Specifically, we evaluate the performance of Leaky Integrate-and-Fire (LIF) neurons within a Convolutional Spiking Neural Network (CSNN). Additionally, we compare two encoding strategies- rate and temporal encoding- to assess their effectiveness in capturing MRI features. The temporal encoding CSNN achieved 73.10% accuracy, showing competitive performance with conventional CNNs while delivering up to 73% memory savings and 13 times faster inference. These results establish the viability of SNNs for MRI analysis, offering valuable insights into their computational efficiency and biological plausibility for resource-constrained clinical environments.**

***Index Terms*—Spiking Neural Networks (SNNs), Brain Tumor Detection, MRI Classification, Neuromorphic Computing, Energy-Efficient AI**

I. Introduction

Magnetic resonance imaging plays an important role in tumor detection. Conventional convolutional neural networks do achieve high accuracy, but are computationally expensive and lack biological plausibility. Additionally, CNNs require substantial energy consumption, making them challenging to deploy in resource-constrained clinical environments. Thus, spiking neural networks offer an alternative to traditional architecture, by mimicking the event-driven nature of biological neurons, thereby identifying patterns efficiently and dynamically, while using reduced compute.

Unlike traditional Artificial Neural Networks (ANNs), SNNs process information through discrete spikes, closely resembling neuronal communication in the human brain. Since SNNs better emulate the way biological neurons communicate through their event-driven sparse spiking-based model, they offer enhanced biological plausibility for neural computation. This spike-based processing enables inherent noise robustness, a critical advantage for MRI data which often contains artifacts from patient movement and magnetic field inhomogeneities. This allows them to encode spatial and temporal dependencies, making them suitable for MRI classification [1] [2] [3]. Additionally, their sparse and asynchronous processing reduces computational overhead significantly compared to traditional CNNs, while enabling real-time processing capabilities [4].

Though convolutional neural networks have been primarily used for MRI image analysis for the advantages that CNNs offer, in this work we investigate the suitability of Convolutional Spiking Neural Networks (CSNNs). This study investigates the effectiveness of SNNs for MRI classification by evaluating the Leaky Integrate-and-Fire (LIF) neuron within CSNNs. Furthermore, the impact of rate and temporal encoding on classification performance is analyzed. By demonstrating the viability of SNN-based approaches, this work highlights their potential advantages in computational efficiency and medical diagnostics.

II. Spiking Neural Networks

SNNs are a class of biologically inspired neural networks. These process information through discrete events that are called spikes. Since they leverage the spikes for computation, they are more energy-efficient than their traditional deep learning counterparts. The main idea behind SNNs is to be able to encode and transmit information using spike trains, exactly the way biological neurons communicate. One of the most common neuron models in SNNs is the Leaky-Integrate-and-Fire Model (LIF), which captures the dynamics of a neuron's membrane potential over time and determines the spiking behavior. This membrane potential is modeled by the differential equation:

$$\tau_m \frac{dV(t)}{dt} = -(V(t) - V_{\text{rest}}) + RI(t)$$

Where, τ_m is the membrane time constant, V_{rest} is the resting potential of the neuron, R is the membrane resistance, and $I(t)$ is the input current.

Here, if the membrane potential $V(t)$ reaches a threshold V_{th}, the neuron will emit a spike, and then the potential is reset to a lower value V_{reset}. Mathematically, this is expressed as:

$$V(t) \geq V_{\text{th}} \Rightarrow \text{Spike occurs, and } V(t) \rightarrow V_{\text{reset}}$$

The LIF model also introduces a leak term $-(V(t) - V_{\text{rest}})$, which ensures that the neuron returns to its resting potential when there is no input.

Convolutional Spiking Neural Networks (CSNNs) build on Convolutional Neural Networks (CNNs) by using spiking neurons. In the CSNN, convolutions are applied followed by

979-8-3315-0266-9/25/$31.00

spiking neuron activations, which makes them efficient for image and video processing. In a CSNN, the convolutional layer extracts features by computing:

$$h_{ij} = \sum_{m,n} W_{mn} \cdot x_{i-m,j-n}$$

where $x_{i,j}$ represents the input feature map, W_{mn} is the convolutional kernel, and h_{ij} is the convolved output. The then convolved features are passed through an SNN layer and converted into spike trains.

III. Related Work

A. Convolutional Neural Networks for MRI Classification

Convolutional neural networks are commonly used for MRI-based tumor detection and classification. This is due to their ability to extract varied features from images [5]. Traditional CNNs, such as AlexNet, VGG, ResNet, and InceptionNet have been used for various medical imaging applications which includes brain tumor detection [6] [7] [8].

These models, however, are very computationally intensive [9] and require significant compute for training and inference. Moreover, traditional CNNs lack biological plausibility, which can be a drawback for researchers interested in understanding brain-like computation. Some approaches may also require manual segmentation of tumor regions [10], which is not fully automated.

B. Spiking Neural Networks in Medical Imaging

SNNs offer a more biologically inspired alternative to traditional convolutional models by mimicking the event-driven nature of biological neurons [19]. Their sparse spike-based communication allows for significant energy efficiency, with studies indicating 10-100 times lower energy consumption compared to conventional neural networks [14]. This efficiency arises from asynchronous activation patterns, which only require computations when membrane potentials reach spiking thresholds [12].

In medical imaging, SNNs have shown promising results [11]:

1) **Brain Tumor Analysis**: Hybrid SNN architectures combining spiking layers with CNNs achieved up to 94.8% accuracy in MRI tumor classification [1], while specialized models improved segmentation by 12% over traditional methods [3]. Evolutionary approaches have enabled precise 3D quantification of tumors in MRI scans [20].
2) **Oncology Imaging**: For breast cancer detection, SNNs utilizing multi-scale saliency fusion reached 96.3% accuracy and reduced computational costs by 38% [13]. In COVID-19 diagnoses, spiking architectures achieved 98.4% sensitivity in detecting lung abnormalities from CT scans [18].
3) **Neurological Signal Processing**: MRI-structured SNNs demonstrated a 20-30% improvement in EEG signal prediction accuracy compared to LSTM models [2]. Real-time implementations have enabled sub-100ms latency in processing functional MRI data streams [16].

Recent advancements address implementation challenges, such as overcoming layer synchronization limitations to improve training convergence by 40% [4]. Adaptive synaptic weight algorithms have enhanced segmentation accuracy on diffusion-weighted MRI scans [17]. Despite these advancements, balancing biological plausibility with computational efficiency remains a challenge, particularly with complex neuron models increasing spiking operations significantly [15].

Continuous learning mechanisms enable real-time model refinement from streaming patient data, positioning SNNs as a transformative technology for medical imaging in resource-constrained environments [19].

C. Neuron Models in SNNs

The choice of neuron model is an important aspect of the performance of an SNN. It has a direct relation to the biological realism and the computational efficiency of the network. Different neuron models vary in their complexity and level of detail [21] [22].

The most commonly used neuron models are:

1) **Leaky Integrate-and-Fire (LIF) Neurons**: LIF neurons are simple and computationally efficient, making them a common choice for large-scale neural networks. They integrate incoming spikes over time and fire when a threshold is reached, resetting afterward. This simplicity allows for fast simulation but may lack the detailed biological accuracy of more complex models [23]
2) **Hodgkin-Huxley (HH) Neurons**: HH neurons are the most biologically realistic since they model the ion channel dynamics of real neurons. However, this comes at the cost of very high computational complexity, limiting their use in large networks [24] [25]
3) **Izhikevich Neurons**: These neurons strike a balance between LIF and HH models by offering both biological realism and computational efficiency. They reproduce firing patterns observed in real neurons, making them versatile for different applications [26]

D. Encoding Schemes

The way that information is encoded in an SNN determines their efficiency and performance in classification. Different methods of encoding process information in different ways, affecting the SNN's ability to capture the spatial and temporal features of the MRI images [27] [30].

1) **Rate Encoding**: Information is encoded by the frequency of spikes over a given time window [28]. It is straightforward in its implementation and is used commonly due to its stability. However, it may not make use of the temporal precision that is innate to spiking computation.
2) **Temporal Encoding**: Unlike rate encoding, this method relies on the timing of the spikes to encode information. This allows more biologically plausible processing and can enhance classification performance. However, this

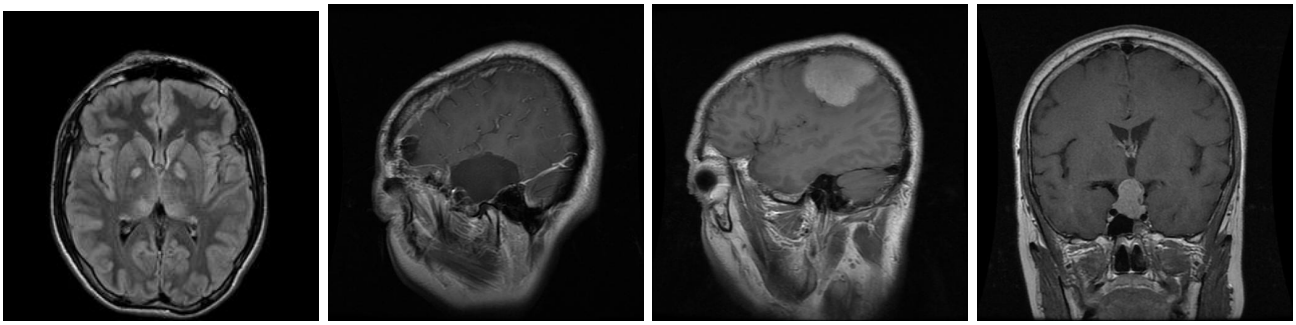

(a) No Tumor (b) Glioma (c) Meningioma (d) Pituitary Tumor

Fig. 1. Example MRI Scans From Four Different Classes in the Dataset

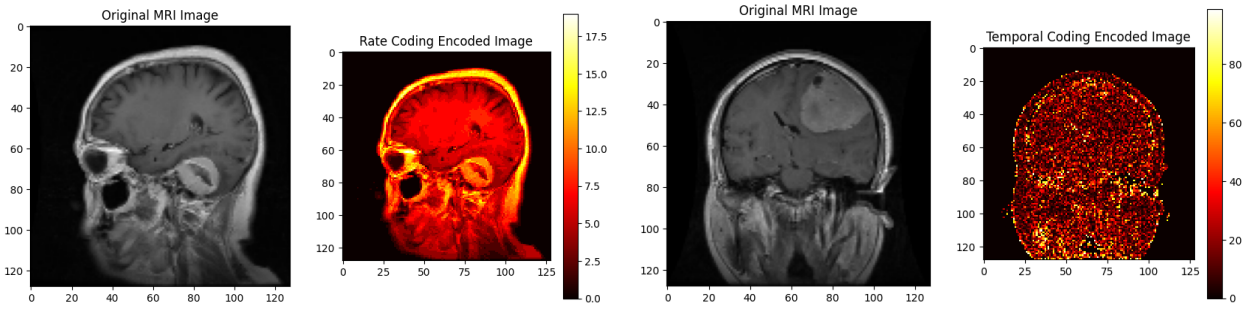

(a) Rate Encoding: Spike Frequency Corresponds to Pixel Intensity (b) Temporal Encoding: Brighter Pixels Spike Earlier in the Time Window

Fig. 2. Comparison of Encoding Methods: Rate Encoding vs Temporal Encoding

method requires more precise spike timing control, which makes it more complex in its implementation [29].

IV. Methodology

A. Data Acquisition and Preprocessing

For this study, the Brain Tumor MRI dataset sourced from Sartaj Bhuvaji's repository was utilized [31], which comprises 3,264 human brain MRI images categorized into four classes: glioma, meningioma, no tumor, and pituitary tumor. The dataset was structured into distinct directories with images resized from 512×512×3 to 150×150×3 dimensions for computational efficiency.

To these images, preprocessing techniques were applied, including normalization by rescaling pixel values to the [0,1] range. Given the critical importance of preserving tumor morphological characteristics, data augmentation was deliberately omitted to maintain the integrity of diagnostic features. The dataset was partitioned using an 88:12 train-test split ratio (approximately 2,870 training and 394 testing images), with the original class distribution maintained to eliminate potential bias.

Samples from each of the four classes are displayed in Figure 1.

B. Convolutional Neural Network Classification

Four distinct CNN architectures were implemented to evaluate their effectiveness in brain tumor classification: EfficientNetB0 [32], TumorDetNet [33], AlexNet [34], and DenseNet201 [35]. Each architecture leverages unique structural advantages for enhanced feature extraction and classification accuracy in medical imaging tasks.

To ensure robust model performance and prevent overfitting, comprehensive regularization strategies were employed, including dropout layers, L2 weight regularization, and batch normalization. Training optimization incorporated early stopping with patience monitoring and adaptive learning rate scheduling based on validation performance. Transfer learning techniques were applied through selective layer freezing, allowing fine-tuning of deeper layers to adapt to MRI-specific morphological features.

All models were trained using categorical cross-entropy loss with the Adam optimizer. Performance assessment included accuracy, precision, recall, F1-score, and AUC-ROC metrics, while computational efficiency was quantified through CPU usage and RAM consumption measurements.

The hyperparameters for each architecture are detailed in Table I.

C. Spiking Neural Network Classification

In order for the SNNs to process MRI images, we use spike-based encoding schemes that convert static MRI images to spike trains. We utilize two common methods- rate and temporal encoding. Both methods translate pixel intensity

TABLE I
HYPERPARAMETERS FOR DIFFERENT CNN ARCHITECTURES

Model	Learning Rate	Epochs	L2 Regularization	Dropout	BatchNorm
EfficientNetB0	0.001	50	1×10^{-5}	0.2	Yes
TumorDetNet	0.0005	100	1×10^{-4}	0.3	Yes
AlexNet	0.01	30	5×10^{-4}	0.5	No
DenseNet201	0.0001	30	1×10^{-5}	0.2	Yes

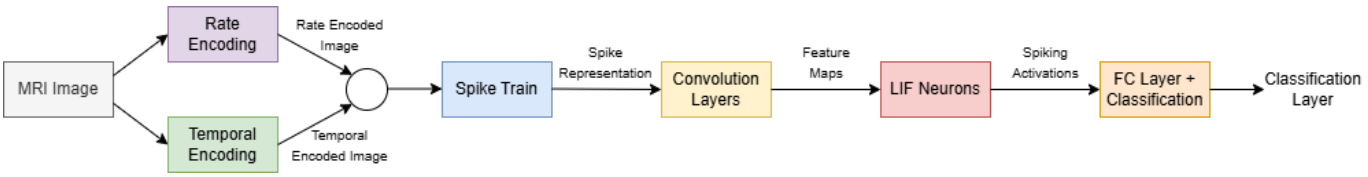

Fig. 3. Architecture of the Convolutional Spiking Neural Network (CSNN)

values to spike patterns that are then processed by the spiking neurons.

1) **Rate Encoding**: This method encodes information by changing the spike frequency relative to the pixel intensity. A higher intensity would correspond to a greater number of spikes within a fixed time window. Conversely, the lower the intensity, the lower the number of spikes. Given an MRI image $\mathbf{I} \in \mathbb{R}^{H \times W}$, where H and W denote height and width, each pixel intensity $I_{ij} \in [0, 1]$ is mapped to a spike train $S_{ij}(t)$ such that:

$$S_{ij}(t) = \begin{cases} 1, & \text{if } t < \lfloor I_{ij} \cdot M \rfloor \\ 0, & \text{otherwise} \end{cases}$$

where M represents the maximum number of spikes per pixel within the predefined time window T. The spike trains are stored as binary tensors of dimension $H \times W \times T$, where T represents the temporal dimension.

2) **Temporal Encoding**: This method uses the precise timing of the spikes to encode pixel intensity. This means that brighter pixels fire earlier in the time window, and darker pixels may fire later or not at all. This helps preserve the temporal dynamics that are important for SNN processing. For a given pixel intensity I_{ij}, spike times t_k are determined as follows:

$$t_k = \lfloor (1 - I_{ij}) \cdot T \rfloor + \epsilon_k$$

where ϵ_k is a small perturbation to introduce biological variability in spike timing.
The resulting spike train consists of sparse and precisely timed events, thereby enabling efficient information representation.
To apply temporal encoding to static MRI images, we mapped each pixel intensity to a single spike event occurring at a specific time step within the window. Brighter pixels triggered spikes at earlier timesteps, while darker pixels fired later. If a pixel had zero intensity, no spike was generated. This encoding transformed a static 2D image into a time-series spike representation, allowing the SNN to process spatial features dynamically over time. The encoded spike matrices were finally stored as .npy files. The results of the rate and temporal encoding are presented in Figure 2.
Both encoding schemes were applied to the MRI images from the aforementioned dataset, and converted the images to spike trains.
To process the input spike trains, we designed a Convolutional Spiking Neural Network (CSNN) optimized for feature extraction and classification. The overall architecture of the proposed model is shown in Figure 3. The network consists of the following key components:

1) **Convolutional Layers**: Two convolutional layers, with 32 and 64 filters, extract the spatial features. Each convolutional layer is followed by an LIF neuron activation and average pooling.
2) **Fully Connected Layers**: A FC layer with 128 neurons processes the extracted features, and is then followed by a dropout layer to prevent overfitting. The final output layer classifies the images.
3) **Leaky Integrate-and-Fire Neurons**: Each layer used LIF Neurons. The purpose was to accumulate input currents over a period of time (the time window was set to 100 timesteps) and fire spikes when a threshold is reached.
SnnTorch 0.9.4 [36] was used for implementing Spiking Neural Networks (SNNs), leveraging its support for neuron models and surrogate gradient learning.
The implementation for the convolutional spiking neural network is described in Table II.

To address reproducibility and statistical validity, all CNN and CSNN models were trained five times with different random seeds, and performance metrics were analyzed across these independent runs. Standard deviations and 95% confidence intervals were calculated using the t-distribution to quantify uncertainty in the reported performance estimates.

TABLE II
PARAMETERS FOR THE CONVOLUTIONAL SPIKING NEURAL NETWORK

Parameter	Value
Learning Rate	0.001
Epochs	30
Batch Size	8
Optimizer	Adam
Loss Function	Cross Entropy
Regularization	Implicit L2 via Adam
Encoding Method	Temporal / Rate
Neuron Model	Leaky-Integrate and Fire
Membrane Decay	0.9
Time Window	100

V. RESULTS AND DISCUSSION

The outcome of the brain tumor classification task by the various convolutional neural network architectures is summarized in Table III. The results of the CSNN with different encoding schemes are summarized in Table IV.

A. Performance Comparison

From the results of our study, we demonstrate that the CSNN achieved comparable, and in some cases, superior performance compared to the traditional CNN counterparts, along with utilizing significantly less memory and computational resources. **The temporal encoding CSNN achieved 73.10% accuracy**, which is competitive with most CNN architectures tested, while the rate encoding CSNN achieved 65.44% accuracy. This highlights the advantages of biologically inspired neural network architectures in resource constrained environments.

The spiking nature of CSNNs allows efficient information encoding and processing through discrete spikes, similar to biological neurons, ensuring neurons only activate when necessary. This event-driven computation occurs only when spikes are present, leading to significant energy savings compared to CNNs that perform dense matrix operations regardless of input sparsity. CSNNs also possess inherent temporal memory through their spiking dynamics, maintaining information about previous inputs without explicit memory modules. This is particularly valuable for MRI analysis where spatial relationships and contextual information are crucial.

B. Encoding Scheme Analysis

The improved performance of temporal encoding over rate encoding (73.10% vs 65.44% accuracy) demonstrates the importance of proper information encoding. Rate encoding places spikes deterministically at the beginning of the time window, creating predictable patterns that underutilize the temporal dimension. Temporal encoding distributes spikes across the entire time window, creating richer temporal patterns and implicit data augmentation where identical pixel intensities generate different temporal signatures, providing more discriminative features and better generalization.

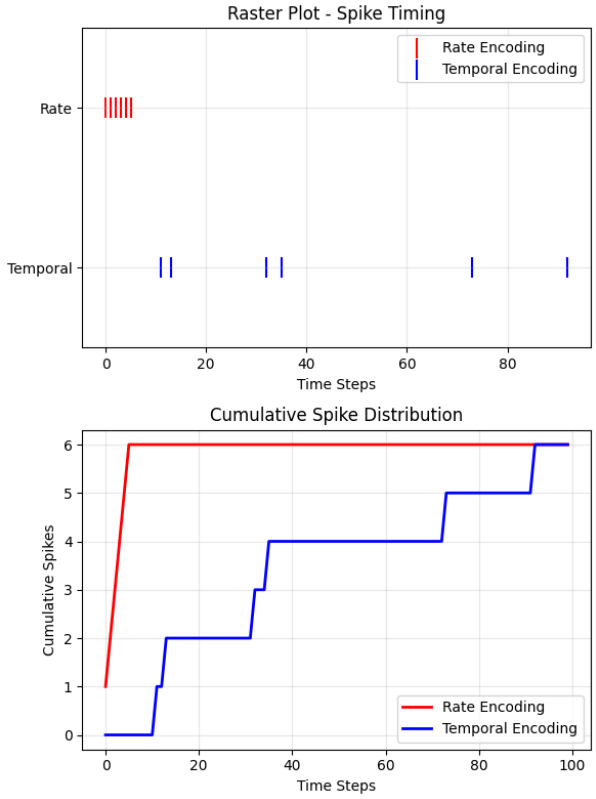

Fig. 4. Comparison of Spike Encoding Schemes Showing Spike Timing and Cumulative Spike Accumulation Over Time

Figure 4 illustrates this difference, showing the spike timing in the raster plot and the spike accumulation over time, highlighting the richer and more distributed temporal patterns achieved through temporal encoding.

C. Biological Advantages and Noise Robustness

CSNNs handle noise and redundant information effectively through spike-based communication, inherently filtering out irrelevant information and focusing on salient features. Their biological inspiration provides robustness to input variations and noise commonly found in medical imaging, with discrete, threshold-based activation mimicking how biological neurons handle noisy inputs. In contrast, CNNs process all input information continuously, potentially leading to overfitting or inefficient feature selection.

D. Resource Efficiency

The resource efficiency of CSNNs is particularly noteworthy. The temporal encoding CSNN utilized 996.72 MB of RAM compared to 3676-6892 MB for CNNs, representing **substantial memory savings of up to 73%**. CPU usage remained at 8.8% while achieving faster inference times of 0.00721 seconds, **over 13 times faster than traditional CNN architectures**. This combination of competitive performance and efficiency makes CSNNs well-suited for deployment in resource-constrained clinical environments.

TABLE III
PERFORMANCE METRICS OF DIFFERENT CNN MODELS

Metric	Value
EfficientNetB0	
Validation Accuracy	62.84% ± 2.45
Mean AUC-ROC	0.808 ± 0.010
Macro Avg Precision	0.653 ± 0.037
Macro Avg Recall	0.623 ± 0.038
Macro Avg F1-Score	0.585 ± 0.032
Avg Inference Time (s)	0.16683
Avg CPU Usage	2.5%
Avg RAM Usage (MB)	4310.96
DenseNet201	
Validation Accuracy	78.68% ± 1.31
Mean AUC-ROC	0.968 ± 0.006
Macro Avg Precision	0.860 ± 0.007
Macro Avg Recall	0.780 ± 0.015
Macro Avg F1-Score	0.758 ± 0.019
Avg Inference Time (s)	0.45777
Avg CPU Usage	48.0%
Avg RAM Usage (MB)	6892.12
AlexNet	
Validation Accuracy	72.84% ± 0.61
Mean AUC-ROC	0.884 ± 0.005
Macro Avg Precision	0.821 ± 0.008
Macro Avg Recall	0.733 ± 0.008
Macro Avg F1-Score	0.693 ± 0.006
Avg Inference Time (s)	0.09688
Avg CPU Usage	23.6%
Avg RAM Usage (MB)	3676.35
TumorDetNet	
Validation Accuracy	61.90% ± 3.20
Mean AUC-ROC	0.837 ± 0.018
Macro Avg Precision	0.728 ± 0.043
Macro Avg Recall	0.603 ± 0.040
Macro Avg F1-Score	0.571 ± 0.055
Avg Inference Time (s)	0.10104
Avg CPU Usage	40.5%
Avg RAM Usage (MB)	5210.22

TABLE IV
PERFORMANCE METRICS OF CSNN WITH DIFFERENT ENCODINGS

Metric	Value
Rate Encoding	
Validation Accuracy	65.44 ± 3.77%
Mean AUC-ROC	0.6990 ± 0.1235
Macro Avg Precision	0.5255 ± 0.2406
Macro Avg Recall	0.5215 ± 0.1527
Macro Avg F1-Score	0.4647 ± 0.1824
Avg Inference Time (s)	0.00699
Avg CPU Usage	4.9%
Avg RAM Usage (MB)	1123.78
Temporal Encoding	
Validation Accuracy	**73.10 ± 0.94%**
Mean AUC-ROC	0.8525 ± 0.0133
Macro Avg Precision	0.7907 ± 0.0114
Macro Avg Recall	0.6670 ± 0.0178
Macro Avg F1-Score	0.6333 ± 0.0236
Avg Inference Time (s)	**0.00721**
Avg CPU Usage	**8.8%**
Avg RAM Usage (MB)	**996.72**

VI. CONCLUSION AND FUTURE WORK

The findings of this study highlight the potential of CSNNs as an effective approach for MRI classification, achieving comparable performance to traditional CNNs while requiring 73% less memory and 13× faster inference. The superior performance of temporal encoding (73.10%) over rate encoding (65.44%) emphasizes the critical importance of proper spike encoding strategies in medical imaging applications. Our CSNN implementation follows fundamental neuromorphic computing principles- spike-based communication, temporal dynamics, and event-driven processing- making it directly compatible with established neuromorphic hardware architectures like Intel Loihi [37] and SpiNNaker [38]. This compatibility positions our approach as a neuromorphic software prototype that can be seamlessly translated to dedicated neuromorphic chips, offering significant advantages for resource-constrained clinical environments.

Future research will focus on validating the generalizability of the proposed CSNN model across multiple medical imaging datasets including BraTS [39] [40] [41], TCIA [42], and other clinical repositories to demonstrate robustness across varying image qualities, acquisition protocols, and tumor types. This multi-dataset evaluation will be essential for establishing clinical applicability beyond single-institution studies. Additionally, we will optimize hybrid encoding techniques and facilitate the transition from our current software implementation to dedicated neuromorphic hardware platforms. The inherent spike-based processing compatibility will enable direct deployment on neuromorphic processors, leveraging their ultra-low power consumption capabilities for integration into portable diagnostic devices and point-of-care clinical workflows, ultimately advancing energy-efficient medical imaging solutions.

REFERENCES

[1] B. Niepceron, A. Nait-Sidi-Moh, and F. Grassia, "Spiking convolutional neural network for brain tumor classification," 2022.

[2] S. A. Saeedinia, M. R. Jahed-Motlagh, A. Tafakhori, and N. Kasabov, "Design of MRI structured spiking neural networks and learning algorithms for personalized modelling, analysis, and prediction of EEG signals," *Scientific Reports*, vol. 11, no. 1, p. 12064, 2021.

[3] Y. Yue et al., "Spiking neural networks fine-tuning for brain image segmentation," *Frontiers in Neuroscience*, vol. 17, p. 1267639, 2023.

[4] R. Koopman, A. Yousefzadeh, M. Shahsavari, G. Tang, and M. Sifalakis, "Overcoming the Limitations of Layer Synchronization in Spiking Neural Networks," *arXiv preprint arXiv:2408.05098*, 2024.

[5] D. Bala et al., "Automated brain tumor classification system using convolutional neural networks from MRI images," in *Proc. 2022 Int. Conf. Eng. Emerging Technol. (ICEET)*, 2022, pp. 1–6.

[6] A. A. Akinyelu et al., "Brain tumor diagnosis using machine learning, convolutional neural networks, capsule neural networks and vision transformers, applied to MRI: a survey," *Journal of Imaging*, vol. 8, no. 8, p. 205, 2022.

[7] M. Talo, O. Yildirim, U. B. Baloglu, G. Aydin, and U. R. Acharya, "Convolutional neural networks for multi-class brain disease detection using MRI images," *Comput. Med. Imaging Graph.*, vol. 78, p. 101673, 2019.

[8] S. D. Ch. and P. Gundagurti, "Deep learning based diagnosis of Parkinson's disease using CNN," *Int. J. Sci. Res. Comput. Sci. Eng. Inf. Technol.*, vol. 6, pp. 351–355, 2020.

[9] P. Maji and R. Mullins, "On the reduction of computational complexity of deep convolutional neural networks," *Entropy*, vol. 20, no. 4, p. 305, 2018.

[10] F. Ullah et al., "Brain tumor segmentation from MRI images using handcrafted convolutional neural network," *Diagnostics*, vol. 13, no. 16, p. 2650, 2023.

[11] X. Li et al., "Review of medical data analysis based on spiking neural networks," *Procedia Comput. Sci.*, vol. 221, pp. 1527–1538, 2023.

[12] K. Yamazaki, V. K. Vo-Ho, D. Bulsara, and N. Le, "Spiking neural networks and their applications: A review," *Brain Sciences*, vol. 12, no. 7, p. 863, 2022.

[13] Q. Fu and H. Dong, "Spiking neural network based on multi-scale saliency fusion for breast cancer detection," *Entropy*, vol. 24, no. 11, p. 1543, 2022.

[14] D. Wu, X. Yi, and X. Huang, "A little energy goes a long way: Build an energy-efficient, accurate spiking neural network from convolutional neural network," *Frontiers in Neuroscience*, vol. 16, p. 759900, 2022.

[15] P. Pietrzak *et al.*, "Overview of spiking neural network learning approaches and their computational complexities," *Sensors*, vol. 23, no. 6, p. 3037, 2023.

[16] J. Kirkland *et al.*, "Imaging from temporal data via spiking convolutional neural networks," *SPIE Proceedings on Medical Imaging and Sensing Technologies*, vol. 11540, pp. 66–85, 2020.

[17] R. Zheng *et al.*, "Image segmentation method based on spiking neural networks with adaptive synaptic weights," *IEEE Signal and Image Processing Conference (ICSIP)*, 2019.

[18] A. Garain, A. Basu, F. Giampaolo, J. D. Velasquez, and R. Sarkar, "Detection of COVID-19 from CT scan images: A spiking neural network-based approach," *Neural Computation and Applications*, vol. 33, no. 19, pp. 12591–12604, 2021.

[19] W. Maass, "Networks of spiking neurons: The third generation of neural network models," *Neural Networks*, vol. 10, no. 9, pp. 1659–1671, Sep. 1997.

[20] A. Baladhandapani and D. S. Nachimuthu, "Evolutionary learning of spiking neural networks towards quantification of 3D MRI brain tumor tissues," *Soft Computing*, vol. 19, pp. 1803–1816, 2015.

[21] M. Ahmadi, A. Sharifi, S. Hassantabar, and S. Enayati, "QAIS-DSNN: tumor area segmentation of MRI image with optimized quantum matched-filter technique and deep spiking neural network," *BioMed Research International*, vol. 2021, no. 1, p. 6653879, 2021.

[22] S. Koravuna et al., "Exploring spiking neural networks: a comprehensive analysis of mathematical models and applications," *Frontiers in Computational Neuroscience*, vol. 17, p. 1215824, 2023.

[23] S. Lu and F. Xu, "Linear leaky-integrate-and-fire neuron model based spiking neural networks and its mapping relationship to deep neural networks," *Frontiers in Neuroscience*, vol. 16, p. 857513, 2022.

[24] X. Fang, S. Duan, and L. Wang, "Memristive Hodgkin-Huxley spiking neuron model for reproducing neuron behaviors," *Frontiers in Neuroscience*, vol. 15, p. 730566, 2021.

[25] U. Chandrashekhar, "The Hodgkin-Huxley Model for Neuron Action Potentials: A Computational Study," *Macalester J. Phys. Astronomy*, vol. 12, no. 1, p. 4, 2024.

[26] E. M. Izhikevich, "Simple model of spiking neurons," *IEEE Trans. Neural Netw.*, vol. 14, no. 6, pp. 1569–1572, 2003.

[27] A. Fois and B. Girau, "Enhanced representation learning with temporal coding in sparsely spiking neural networks," *Frontiers in Computational Neuroscience*, vol. 17, p. 1250908, 2023.

[28] A. A. Al-Hamid and H. Kim, "Optimization of spiking neural networks based on binary streamed rate coding," *Electronics*, vol. 9, no. 10, p. 1599, 2020.

[29] I. M. Comsa et al., "Temporal coding in spiking neural networks with alpha synaptic function," in *Proc. ICASSP 2020 IEEE Int. Conf. Acoust. Speech Signal Process.*, 2020, pp. 8529–8533.

[30] C. Wang et al., "Neural encoding with unsupervised spiking convolutional neural network," *Communications Biology*, vol. 6, no. 1, p. 880, 2023.

[31] A. Kadam, S. Bhuvaji, and S. Deshpande, "Brain tumor classification using deep learning algorithms," *Int. J. Res. Appl. Sci. Eng. Technol.*, vol. 9, pp. 417–426, 2021.

[32] M. Tan and Q. Le, "EfficientNet: Rethinking model scaling for convolutional neural networks," in *Proc. Int. Conf. Mach. Learn.*, 2019, pp. 6105–6114.

[33] N. Ullah et al., "TumorDetNet: A unified deep learning model for brain tumor detection and classification," *PLoS ONE*, vol. 18, no. 9, p. e0291200, 2023.

[34] A. Krizhevsky, I. Sutskever, and G. E. Hinton, "ImageNet classification with deep convolutional neural networks," in *Adv. Neural Inf. Process. Syst.*, vol. 25, 2012.

[35] G. Huang, Z. Liu, L. van der Maaten, and K. Q. Weinberger, "Densely connected convolutional networks," in *Proc. IEEE Conf. Comput. Vis. Pattern Recognit.*, 2017, pp. 4700–4708.

[36] J. K. Eshraghian, M. Ward, E. Neftci, X. Wang, G. Lenz, G. Dwivedi, M. Bennamoun, D. S. Jeong, and W. D. Lu, "Training spiking neural networks using lessons from deep learning," *Proceedings of the IEEE*, vol. 111, no. 9, pp. 1016–1054, 2023.

[37] Davies, M., Srinivasa, N., Lin, T. H., Chinya, G., Cao, Y., Choday, S. H., et al., "Loihi: A Neuromorphic Manycore Processor With On-Chip Learning," *IEEE Micro*, vol. 38, no. 1, pp. 82–99, Jan.–Feb. 2018.

[38] Mayr, C., Hoeppner, S., and Furber, S., "SpiNNaker 2: A 10 Million Core Processor System for Brain Simulation and Machine Learning-Keynote Presentation," in *Communicating Process Architectures 2017 2018*, IOS Press, pp. 277–280, 2019.

[39] B. H. Menze, A. Jakab, S. Bauer, J. Kalpathy-Cramer, K. Farahani, J. Kirby, et al. "The Multimodal Brain Tumor Image Segmentation Benchmark (BRATS)", IEEE Transactions on Medical Imaging 34(10), 1993-2024 (2015) DOI: 10.1109/TMI.2014.2377694

[40] S. Bakas, H. Akbari, A. Sotiras, M. Bilello, M. Rozycki, J.S. Kirby, et al., "Advancing The Cancer Genome Atlas glioma MRI collections with expert segmentation labels and radiomic features", Nature Scientific Data, 4:170117 (2017) DOI: 10.1038/sdata.2017.117

[41] S. Bakas, M. Reyes, A. Jakab, S. Bauer, M. Rempfler, A. Crimi, et al., "Identifying the Best Machine Learning Algorithms for Brain Tumor Segmentation, Progression Assessment, and Overall Survival Prediction in the BRATS Challenge", arXiv preprint arXiv:1811.02629 (2018)

[42] Schmainda KM, Prah M (2018). Data from Brain-Tumor-Progression. The Cancer Imaging Archive. https://doi.org/10.7937/K9/TCIA.2018.15quzvnb